Mon. Not. R. Astron. Soc. **389,** 1453–1460 (2008) doi:10.1111/j.1365-2966.2008.13683.x

Can a primordial magnetic field originate large-scale anomalies in *WMAP* data?

A. Bernui[1⋆] and W. S. Hipólito-Ricaldi[2⋆]

[1] *Instituto Nacional de Pesquisas Espaciais, Divisão de Astrofísica, Av. dos Astronautas 1758, 12227-010 – São José dos Campos, SP, Brazil*
[2] *Universidade Federal do Espírito Santo, Departamento de Física, 29060-900 – Vitória, ES, Brazil*

Accepted 2008 July 4. Received 2008 July 3; in original form 2008 June 3

ABSTRACT

Several accurate analyses of the cosmic microwave background (CMB) temperature maps from the Wilkinson Microwave Anisotropy Probe (*WMAP*) have revealed a set of anomalous results, at large angular scales, that appears inconsistent with the statistical isotropy expected in the concordance cosmological model Λcold dark matter. Because these anomalies seem to indicate a preferred direction in the space, here we investigate the signatures that a primordial magnetic field, possibly present in the photon–baryon fluid during the decoupling era, could have produced in the large-angle modes of the observed CMB temperature fluctuations maps. To study these imprints, we simulate Monte Carlo CMB maps, which are statistically anisotropic due to the correlations between CMB multipoles induced by the magnetic field. Our analyses reveal the presence of the north–south angular correlations asymmetry phenomenon in these Monte Carlo maps, and we use these information to establish the statistical significance of such phenomenon observed in *WMAP* maps. Moreover, because a magnetic field produces planarity in the low-order CMB multipoles, where the planes are perpendicular to the preferred direction defined by the magnetic field, we investigate the possibility that two CMB anomalous phenomena, namely the north–south asymmetry and the quadrupole–octopole planes alignment, could have a common origin. Our results, for large angles, show that the correlations between low-order CMB multipoles introduced by a sufficiently intense magnetic field, can reproduce some of the large-angle anisotropic features mapped in *WMAP* data. We also reconfirm, at more than 95 per cent CL, the existence of a north–south power asymmetry in the *WMAP* 5-yr data.

Key words: cosmic microwave background – cosmology: observations.

1 INTRODUCTION

The 5-yr data from the Wilkinson Microwave Anisotropy Probe (*WMAP*) (Dunkley et al. 2008; Gold et al. 2008; Hinshaw et al. 2008; Komatsu et al. 2008; Nolta et al. 2008) contain the most valuable cosmological information to study the large-scale properties of the Universe (see Bennett et al. 2003a,b; Hinshaw et al. 2003a,b, 2007; Jarosik et al. 2007; Spergel et al. 2007 for previous releases of *WMAP* data). One of these features concerns the hypothesis that the set of temperature fluctuations of the cosmic microwave background (CMB) radiation is a stochastic realization of a random field, meaning that its angular distribution on the celestial sphere is statistically isotropic at all angular scales. Examination of the 3-yr *WMAP* data confirms highly significant departures from statistical isotropy at large angular scales (Abramo et al. 2006a; Huterer 2006; Vielva et al. 2006; Wiaux et al. 2006; Bernui et al. 2007b; Copi et al. 2007; Eriksen et al. 2007; Land & Magueijo 2007; Park, Park & Gott III 2007; Vielva et al. 2007), previously found also in first-year *WMAP* data (Tegmark, de Oliveira-Costa & Hamilton 2003; Bielewicz, Górski & Banday 2004; Copi, Huterer & Starkman 2004; de Oliveira-Costa et al. 2004; Eriksen et al. 2004a; Hansen, Banday & Górski 2004a; Hansen et al. 2004b; Eriksen et al. 2005; Land & Magueijo 2005a,b; Bernui et al. 2006a; Copi et al. 2006). Evidences for such large-angle anisotropy come from the asymmetry of the CMB angular correlations between the northern and southern ecliptic hemispheres (hereafter NS-asymmetry), with indications of a preferred axis of maximum hemispherical asymmetry (Bielewicz et al. 2004; Hansen et al. 2004a,b; Eriksen et al. 2004a, 2005; Land & Magueijo 2005a,b; Bernui et al. 2006a, 2007b, 2007c; Eriksen et al. 2007; Land & Magueijo 2007). Furthermore, other manifestations of large-angle anisotropy include the unlikely quadrupole–octopole planes alignment (referring both to the strong planarity of these multipoles as well as to the alignment between such planes, see e.g. Tegmark et al. 2003; de Oliveira-Costa et al. 2004; Weeks 2004; Abramo et al. 2006a; Copi et al. 2006; Wiaux et al. 2006; Copi et al.

⋆E-mail: bernui@das.inpe.br (AB); hipolito@cce.ufes.br (WSH)

2007; Park et al. 2007). Actually, several anomalous results were already reported after analyses of the *WMAP* data (Chiang et al. 2003; Copi, Huterer & Starkman 2004; Vielva et al. 2004; Bielewicz et al. 2005; Cruz et al. 2005; Bernui, Tsallis & Villela 2006b; McEwen et al. 2006; Bernui, Tsallis & Villela 2007a; Cruz et al. 2007). For a different point of view, see e.g. Hajian & Souradeep (2003), Hajian, Souradeep & Cornish (2004), Donoghue & Donoghue (2005), Souradeep & Hajian (2004), Hajian & Souradeep (2005), Souradeep & Hajian (2005), Souradeep, Hajian & Basak (2006) and Hajian & Souradeep (2006).

Possible sources of these anomalies include non-CMB contaminants, like residual foregrounds (Eriksen et al. 2004b; Wibig & Wolfendale 2005; Abramo, Sodré & Wuensche 2006b; Cruz et al. 2006; de Oliveira-Costa & Tegmark 2006; Chiang et al. 2007; López-Corredoira 2007), incorrectly subtracted dipole and/or dynamic quadrupole terms (Copi et al. 2006; Helling, Schupp & Tesileanu 2006; Copi et al. 2007) or systematic errors (Schwarz et al. 2004; Bunn et al. 2007). For this, particular efforts have been done by the *WMAP* team in last releases in order to improve the data processing by minimizing the effects of foregrounds (mainly coming from diffuse Galactic emission and astrophysical point sources), artefacts (in the map making process, in the instrument characterization, etc.), and systematic errors (Jarosik et al. 2007; Gold et al. 2008; Hinshaw et al. 2008). As a result, the data released by the *WMAP* team include the Internal Linear Combination (hereafter ILC-5 yr) full-sky CMB map suitable for large-angle temperature fluctuations studies (Hinshaw et al. 2007, 2008; Nolta et al. 2008). Here, we investigate the ILC-5yr map, and for completeness, we also study the other full-sky cleaned CMB maps that were differently processed from *WMAP* 5- and 3-yr data releases in order to account for foregrounds and systematics. Thus, we also consider the Kim–Naselsky–Christensen (Kim, Naselsky & Christensen 2008), *WMAP*-3 yr ILC (Hinshaw et al. 2007), de Oliveira–Tegmark (de Oliveira-Costa & Tegmark 2006) and Park–Park–Gott (Park et al. 2007) CMB maps, hereafter termed the HILC-5 yr, ILC-3 yr, OT-3 yr and PPG-3 yr, respectively.

A number of studies have been done looking for physical explanations of the above mentioned anomalies, specially searching for a unifying mechanism relating both the NS-asymmetry and the CMB lower multipoles alignment (see e.g. Wiaux et al. 2006; Dvorkin, Peiris & Hu 2007; Rakic & Schwarz 2007). Additionally, some processes that breaks down statistical isotropy during the inflationary epoch have been suggested (Gordon et al. 2005; Ackerman, Carrol & Wise 2007; Donoghue, Dutta & Ross 2007; Gümrükçüoğlu, Contaldi & Peloso 2007; Koivisto & Mota 2008a, 2008b; Pullen & Kamionkowsi 2007; Pitrou, Pereira & Uzan 2008). Nonetheless, one can also interpret such CMB large-angle anisotropy as being of cosmological origin, in this sense globally axisymmetric space–times have been proposed to account for the mapped preferred axis in *WMAP* maps (Aurich, Lustin & Steiner 2005; Campanelli, Cea, Tedesco 2006; Cresswell et al. 2006; Jaffe et al. 2006; Land & Magueijo 2006; Campanelli, Cea, Tedesco 2007; Gosh, Hajian & Souradeep 2007; Pereira, Pitrou & Uzan 2007). Previous works investigated the effects of a primordial homogeneous magnetic field on the CMB temperature fluctuations on all angular scales (see e.g. Durrer, Kahniashvili & Yates 1998; Demiański & Doroshkevich 2007). Here, we study such primordial field as a possible physical mechanism to produce two large-angle phenomena, that is, the CMB NS asymmetry and the lower CMB multipoles alignment.

In Section 2, we present this primordial magnetic field scenario, and show the effect of such a field on the CMB temperature fluctuations. Then, in order to reveal such effects on simulated CMB maps, we develop a geometrical–statistical method, which is presented in Section 3. After that we use our anisotropic indicator to perform, in Section 4, the analyses of both sets of data, the Monte Carlo (MC) simulated CMB maps as well as the *WMAP* maps. At the end, in Section 5, we discuss our results and formulate our conclusions.

2 PRIMORDIAL MAGNETIC FIELDS SCENARIO

There is strong observational evidence for the presence of large-scale intergalactic magnetic fields of few μG, and magnetic fields of similar strength within clusters of galaxies (see e.g. Krause, Beck & Hummel 1989; Wolfe, Lanzetta & Oren 1992; Clarke, Kroenberg & Boehringer 2001; Widrow 2002; Xu et al. 2006). Nowadays, it is believed that these magnetic fields are amplifications of small primordial magnetic fields of the order of few nanoGauss, that would have occurred due to different processes, like galactical dynamo (see e.g. Parker 1971; Vainshtein & Ruzmaikin 1972; Vainshtein & Zel'dovich 1972), during anisotropic protogalactic collapses, or due to differential rotation in galaxies (see e.g. Piddington 1970; Kulsrud & Anderson 1992). In turn, such primordial seeds of magnetic fields would have several origins, for instance an electroweak phase transition (Vachaspati 1993; Kibble & Vilekin 1995; Baym, Bodeker & McLerran 1996) or quark-hadron phase transition (see e.g. Quashnock, Loeb & Spergel 1989; Cheng & Olinto 1994). Here, we assume the existence of a primordial homogeneus magnetic field and investigate their effects on the CMB temperature fluctuations at large angles.

According to the Einstein equations for linearized metric perturbations, in absence of a magnetic field, the vector metric perturbations go like a^{-2} and the velocity induced by these perturbations goes like a^{-1} (where a is the scale factor that accounts for the expansion of the Universe). Therefore, they decay very fast with the expansion of the Universe (Mukhanov 2005) and the velocities produced by vector metric perturbations do not contribute significatively to the CMB temperature fluctuations.

The presence of a homogeneus magnetic field in the early Universe changes this scenario because such fields modify the behaviour of charged particles in the primordial plasma via Lorentz forces producing additional velocity gradients in the fluid. In this way, a magnetic field induces Alfvén waves in the primordial plasma that propagate at velocity $v_{\rm A}$, changing the speed of sound in the photon–baryon fluid as $c_s^2 \longrightarrow c_s^2 + v_{\rm A}^2 \cos^2\theta$, where (Adams et al. 1996)

$$v_{\rm A}^2 = \frac{B_0^2}{4\pi(\rho + p)}, \tag{1}$$

with ρ and p being the density and pressure in the radiation dominated era, respectively, B_0 is the strength of the magnetic field $\boldsymbol{B}$, θ is the angle between $\boldsymbol{B}$ and the $\boldsymbol{k}$ mode of the Fourier expansion of Alfvén velocity $v_{\rm A}$. These Alfvén wave modes induce small rotational velocity perturbations which, for the scales of our interest, have the form $\boldsymbol{v} \approx \boldsymbol{v}_0\, v_{\rm A}\, k\, t \cos\theta$, where t is the cosmic time, $k \equiv |\boldsymbol{k}|$ and $\boldsymbol{v}_0$ is the initial velocity, which we assume to have a power spectrum of the form (Durrer et al. 1998; Chen et al. 2004)

$$\langle v_{0i}\, v_{0j} \rangle \propto k^n\, (\delta_{ij} - k_i\, k_j). \tag{2}$$

Vectorial contributions to CMB temperature fluctuations are present via Doppler and Sachs–Wolfe effects (Durrer et al. 1998)

$$\frac{\delta T}{T}(\hat{n})^{(\rm vec)} = -\boldsymbol{V}_T \cdot \hat{n}\big|_{t_{\rm dec}}^{t_0} + \int_{t_{\rm dec}}^{t_0} \dot{\boldsymbol{v}} \cdot \hat{n}\, {\rm d}t, \tag{3}$$

where $\hat{n}$ indicates any direction in the sky, $\boldsymbol{V}_T = \boldsymbol{V} + \boldsymbol{v}$, $\boldsymbol{v}$ is the vectorial metric perturbation, $\boldsymbol{V}$ is the velocity produced by $\boldsymbol{v}$ and the integration is between the actual time t_0 and the decoupling time $t_{\rm dec}$. Thus, only the rotational velocity perturbations $\boldsymbol{v}$ contributes effectively to temperature fluctuations because $\boldsymbol{v}$ and $\boldsymbol{V}$ decay quickly with the expansion of the Universe (Mukhanov 2005). Therefore, the signatures of a homogeneus primordial magnetic field $\boldsymbol{B}$ on the CMB temperature fluctuations are (Durrer et al. 1998)

$$\frac{\delta T}{T}^{\boldsymbol{B}}(\hat{n}, k) \approx \hat{n} \cdot \boldsymbol{v}_0\, v_A\, k\, t_{\rm dec}\, \cos\theta. \tag{4}$$

As we can see, the existence of a preferred direction associated to $\boldsymbol{B}$ affects the CMB temperature fluctuations through the angle θ, which implies, a straight dependence on the orientation of the vector $\boldsymbol{B}$, consequently, a break down of the statistical isotropy in the CMB sky.

The most suitable quantity to simulate statistically anisotropic CMB skies is the correlation matrix of multipole coefficients. For this, we expand the sky temperature fluctuations in spherical harmonics:

$$\frac{\delta T}{T}(\hat{n}) = \sum_{\ell,m} a_{\ell m} Y_{\ell m}(\hat{n}), \tag{5}$$

$$a_{\ell m} = \int \frac{\delta T}{T}(\hat{n})\, Y^*_{\ell m}(\hat{n})\, {\rm d}\Omega, \tag{6}$$

and then use equations (2)–(5) to calculate the correlation matrix $[a_{\ell m}\, a^*_{\ell' m'}]$. In this work, we assume a scale-invariant power spectrum for the magnetic field, i.e. $n = -5$ in the equation (2).

The explicit calculation of the correlation matrix elements, for a Harrison–Zel'dovich scale-invariant power spectrum for the magnetic field, gives (Durrer et al. 1998; Chen et al. 2004; Naselsky & Kim 2008)

$$\langle a_{\ell m} a^*_{\ell' m'} \rangle^{\boldsymbol{B}} = \delta_{mm'} \left[\delta_{\ell\ell'} C^{\boldsymbol{B}}_{\ell m} + (\delta_{\ell+1,\ell'-1} + \delta_{\ell-1,\ell'+1}) D^{\boldsymbol{B}}_{\ell m} \right], \tag{7}$$

where

$$C^{\boldsymbol{B}}_{\ell m} = 27.12 \times 10^{-16} \left(\frac{B_0}{1\,{\rm nG}} \right)^4 \times \frac{2\ell^4 + 4\ell^3 - \ell^2 - 3\ell + 6m^2 - 2\ell m^2 - 2\ell^2 m^2}{(\ell+2)(\ell+1)\ell(\ell-1)(2\ell-1)(2\ell+3)} \tag{8}$$

and

$$\frac{D^{\boldsymbol{B}}_{\ell m}}{C^{\boldsymbol{B}}_{\ell m}} = \frac{9\pi}{32} \frac{\sqrt{(\ell+m+1)(\ell-m+1)(\ell+m)(\ell-m)}}{2\ell^4 + 4\ell^3 - \ell^2 - 3\ell + 6m^2 - 2\ell m^2 - 2\ell^2 m^2} \times \frac{\sqrt{(2\ell-1)(2\ell+3)}(\ell-1)(\ell+2)}{(2\ell+1)} \tag{9}$$

noting that B_0 is given in nanoGauss (nG). Thus, the computation of the correlation matrix leads to non-zero elements of the type $(\ell, m) = (\ell', m')$ and $(\ell, m) = (\ell' \pm 2, m')$, while all the other elements are zero. In other words, the multipole matrix correlation is non-diagonal which is an inheritance of its angular dependence on θ and $\boldsymbol{v}_0$, shown in the equation (4), and this fact being a consequence of the presence of the magnetic field at early times. In this scenario, correlations appear between different scales, like ℓ and $\ell \pm 2$, and then the multipole coefficients $a_{\ell m}$ at such scales are correlated. For this reason, one concludes that large-angle anisotropy features should appear in the CMB maps produced by this primordial magnetic field. If we consider a magnetic field in a Λcold dark matter (ΛCDM) Universe, the correlation matrix will be

$$\langle a_{\ell m} a^*_{\ell' m'} \rangle = \langle a_{\ell m} a^*_{\ell' m'} \rangle^{\Lambda{\rm CDM}} + \langle a_{\ell m} a^*_{\ell' m'} \rangle^{\boldsymbol{B}}, \tag{10}$$

where

$$\langle a_{\ell m} a^*_{\ell' m'} \rangle^{\Lambda{\rm CDM}} = C^{\Lambda{\rm CDM}}_{\ell}\, \delta_{mm'}\, \delta_{\ell\ell'}. \tag{11}$$

We observe that correlations between temperature fluctuations do not only depend on the angular separation between two points, but also on their orientation with respect to the magnetic field, that is, m-dependence. This m-dependence, caused by the fact that $B_0 \neq 0$, means that now the CMB temperature fluctuations are actually statistically anisotropic.

Our purpose here is just to illustrate the effect induced by these large-angle anisotropies in CMB maps, and compare them with those features found in the CMB maps from *WMAP*. To study the relationship between low ℓ (i.e. from $\ell = 2$ to 10) anomalies in such anisotropic magnetic field scenario, we produce, according to equations (7)–(11), five sets (with different strengths B_0) of MC-simulated CMB maps. For the statistically isotropic part (i.e. the first term in equation 10), we use the CMBFAST tool to calculate the angular power spectrum $C^{\Lambda{\rm cdm}}_{\ell}$, and after that we use Cholesky decomposition of the matrix (10) in order to deal with the non-diagonality. Then, we randomically simulate the $a_{\ell m}$ coefficient sets and from them we generate the CMB temperature fluctuations maps. The simulations were performed for magnetic fields intensities $B_0 = (20 \pm 10)$ nG, to be in agreement with known limits at cosmological scales for the $n = -5$ power spectrum (see e.g. Barrow, Ferreira & Silk 1997; Chen et al. 2004; Naselsky & Kim 2008, and Kahniashvili, Maravin & Kosowsky 2008 for other power spectrum indices).

3 THE 2PACF AND THE σ-MAP METHOD

Our method to investigate the large-scale angular correlations in CMB temperature fluctuations maps consists in the computation of the two-point angular correlation function (2PACF) (Padmanabhan 1993) in a set of spherical caps covering the celestial sphere.

Let $\Omega^J_{\gamma_0} \equiv \Omega(\theta_J, \phi_J; \gamma_0) \subset \mathcal{S}^2$ be a spherical cap region on the celestial sphere, of γ_0 degrees of aperture, with vertex at the Jth pixel, $J = 1, \ldots, N_{\rm caps}$, where (θ_J, ϕ_J) are the angular coordinates of the Jth pixel's centre. Both, the number of spherical caps $N_{\rm caps}$ and the coordinates of their centres (θ_J, ϕ_J), are defined using the HEALPix pixelization scheme (Górski et al. 2003). The union of the $N_{\rm caps}$ spherical caps covers completely the celestial sphere $\mathcal{S}^2$.

Given a pixelized CMB map, the 2PACF of the temperature fluctuations δT corresponding to the pixels located in the spherical cap $\Omega^J_{\gamma_0}$ is defined by (Padmanabhan 1993)

$$\mathrm{C}(\gamma)^J \equiv \langle\, \delta T(\theta_i, \phi_i) \delta T(\theta_{i'}, \phi_{i'})\, \rangle, \tag{12}$$

where $\cos\gamma = \cos\theta_i \cos\theta_{i'} + \sin\theta_i \sin\theta_{i'} \cos(\phi_i - \phi_{i'})$, and $\gamma \in (0, 2\gamma_0]$ is the angular distance between the ith and the i'th pixels centres. The average $\langle\ \rangle$ in the above equation is done over all the products $\delta T(\theta_i, \phi_i)\, \delta T(\theta_{i'}, \phi_{i'})$ such that $\gamma_k \equiv \gamma \in ((k-1)\delta, k\delta]$, for $k = 1, \ldots, N_{\rm bins}$, where $\delta \equiv 2\gamma_0 / N_{\rm bins}$ is the binwidth. We denote by $\mathrm{C}^J_k \equiv \mathrm{C}\,(\gamma_k)^J$ the value of the 2PACF for the angular distances $\gamma_k \in (k-1)\delta, k\delta]$. Define now the scalar function $\sigma : \Omega^J_{\gamma_0} \subset \mathcal{S}^2 \mapsto \Re^+$, for $J = 1, \ldots, N_{\rm caps}$, which assigns to the J-cap, centred at (θ_J, ϕ_J), a real positive number $\sigma_J \equiv \sigma(\theta_J, \phi_J) \in \Re^+$. The most natural way of defining a measure σ is through the variance of the C^J_k function (Bernui et al. 2007b),

$$\sigma^2_J \equiv \frac{1}{N_{\rm bins}} \sum_{k=1}^{N_{\rm bins}} (\mathrm{C}^J_k)^2. \tag{13}$$

To obtain a quantitative measure of the angular correlations in a CMB map, we cover the celestial sphere with $N_{\rm caps}$ spherical caps,

and calculate the set of σ values $\{\sigma_J, J = 1, \ldots, N_{\rm caps}\}$ using the equation (13). Associating the Jth σ value σ_J to the Jth pixel, for $J = 1, \ldots, N_{\rm caps}$, one fills the celestial sphere with positive real numbers, and according to a linear scale (where $\sigma^{\rm minimum} \rightarrow$ blue, $\sigma^{\rm maximum} \rightarrow$ red), one converts this numbered map into a coloured map: this is the σ-map. Finally, we find the multipole components of a σ-map by calculating its angular power spectrum. In fact, given a σ-map one can expand $\sigma = \sigma(\theta, \phi)$ in spherical harmonics: $\sigma(\theta, \phi) = \sum_{\ell, m} A_{\ell m} Y_{\ell m}(\theta, \phi)$. Then, the set of values $\{S_\ell, \ell = 1, 2, \ldots\}$, where $S_\ell \equiv [1/(2\ell + 1)] \sum_{m=-\ell}^{\ell} |A_{\ell m}|^2$, give the angular power spectrum of the σ-map.

A power spectrum $S^{WMAP}{}_\ell$ of a σ-map computed from a given *WMAP* map, provides quantitative information about large-angle anisotropy features of such a CMB map when compared with the mean of σ-map power spectra obtained from MC CMB maps produced under the statistical isotropy hypothesis. As we will see, the σ-map analysis is able to reveal large-angle anisotropies such as the NS-asymmetry.

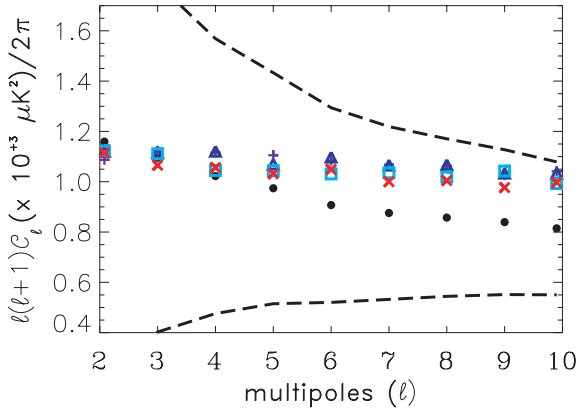

Figure 1. Normalized mean angular power spectra of the MC CMB maps used to produce the σ-maps–MC. The bullet, plus, triangle, square and times symbols represent the data when $B_0 = 0, 10, 15, 20, 30$ nG, respectively. The dashed lines are the cosmic variance limits of the ΛCDM (i.e. $B_0 = 0$) power spectrum case. Note that the four sets of MC maps with $B_0 \neq 0$ have their angular power spectra consistent with the ΛCDM case.

4 DATA ANALYSES AND RESULTS

Now we will apply the σ-map method to scrutiny the large-angle correlations present in the *WMAP* maps, and perform a quantitative comparison with the result of a similar analysis performed in sets of simulated MC CMB maps. These sets of simulated maps are produced according to the primordial magnetic field scenario discussed above, where we consider five cases, for an equal number of values for the parameter B_0, to examine the influence of the field intensity on the CMB angular correlations. These analyses let us to test the hypothesis that the anomalous angular correlations found in the *WMAP* data could be explained by the presence of a magnetic field acting in the decoupling era. The *WMAP* data under investigation are the full-sky cleaned CMB maps derived from *WMAP* 3- and 5-yr releases, namely the ILC-5 yr, HILC-5 yr, ILC-3 yr, OT-3 yr and PPG-3 yr CMB maps. Because we are interested to understand the possible cause–effect relationship between a primordial magnetic field and the large-angle anomalies mapped in CMB *WMAP* data, we concentrate our study on the low-order multipoles range $\ell = 2$– 10.

For our analyses, we produce five sets of 1000 MC CMB maps each, corresponding to the cases when $B_0 = 0, 10, 15, 20$ and 30 nG. The case $B_0 = 0$ means that the MC maps were generated using a pure ΛCDM angular power spectrum seed (Spergel et al. 2007; Komatsu et al. 2008), and this case refers to the statistically isotropic CMB maps.

For $B_0 \neq 0$, the simulated MC CMB maps were produced considering the two contributions to the random $a_{\ell m}$ modes according to equation (10), that is, the statistically isotropic part plus the component due to the magnetic field. As a result of this, the mean angular power spectra of each set of MC maps, for $B_0 = 10, 15, 20, 30$ nG, satisfy the Sachs–Wolfe plateau effect. However, due to the contributions $[a_{\ell m} a^*_{\ell' m'}]^{\boldsymbol{B}}$ (see the second term in equation 10) the plateau of these mean angular power spectra are shifted upwards, where the value of such shifts is proportional to B_0. In order to compare features obtained, through the σ-map method, from MC maps with power spectra that be consistent with the ΛCDM power spectrum, we normalize the MC power spectra corresponding to the $B_0 \neq 0$ cases. The normalized mean angular power spectra C_ℓ of these four sets of MC maps $B_0 \neq 0$ cases and the angular power spectrum of the ΛCDM model, plus its cosmic variance limits, are shown in Fig. 1.

In our simulations, we have assumed that the magnetic field is pointing in the South Galactic Pole–North Galactic Pole (SGP–NGP) direction. Note that all the sky maps plotted here are in Galactic coordinates, which means that the equator of the map corresponds to the Galactic plane, and the axis SGP–NGP is perpendicular to this plane.

The data analyses consist on the following steps. For each MC temperature map, we compute its corresponding σ-map (hereafter called σ-map–MC), and then we calculate its angular power spectrum $\{S_\ell, \ell = 1, 2, \ldots\}$. The statistical significance of the σ-map angular power spectra computed from *WMAP* data (hereafter called σ-map–*WMAP*) comes from the comparison with the five sets of 1000 angular power spectra obtained from the σ-maps–MC. To illustrate the effect of the magnetic field in the CMB low-order multipoles in MC maps, we show three cases in Fig. 2: the mean of 100 σ-maps–MC obtained from a similar number of MC computed considering the statistically isotropic case $B_0 = 0$ nG (top panel), and considering magnetic field intensities $B_0 = 10$ nG (middle panel) and $B_0 = 30$ nG (bottom panel), respectively. In Fig. 3 instead, we show three σ-maps with large value of the dipole term S_1, indicative of the hemispherical asymmetry phenomenon, produced from the ILC-5 yr map (top panel) and from MC CMB maps with different magnetic field intensities: $B_0 = 10$ nG (middle panel) and $B_0 = 30$ nG (bottom panel).

In Fig. 4, we present the results of the σ-maps spectra analyses. We observe that the σ-maps–*WMAP*, obtained from the ILC-5 yr, HILC-5 yr, ILC-3 yr, OT-3 yr and PPG-3 yr CMB maps, reveal a dipole moment $S_1^{\rm wmap}$ larger than 95 per cent of the values $S_1^{\rm MC-\Lambda CDM}$, corresponding to σ-maps–MC obtained from statistically isotropic CMB maps. This fact indicates that the NS-asymmetry phenomenon is present in *WMAP* data at 95 per cent CL. However, we also observe in Fig. 4 that the angular power spectra of the σ-maps–MC vary with the magnetic field intensity, thus to larger values of B_0 correspond σ-maps–MC with larger values of the terms S_1 (dipole), S_2 (quadrupole), S_3 (octopole), etc. In other words, a larger value of B_0 produces a stronger hemispherical asymmetry in the MC CMB maps. Therefore, we conclude that for sufficiently large B_0, one can interpret the spectra resulting from σ-maps–*WMAP* as being not anomalous at all, but consistent with those CMB temperature maps produced according to the primordial magnetic field scenario.

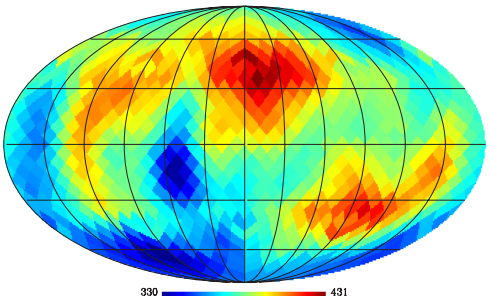

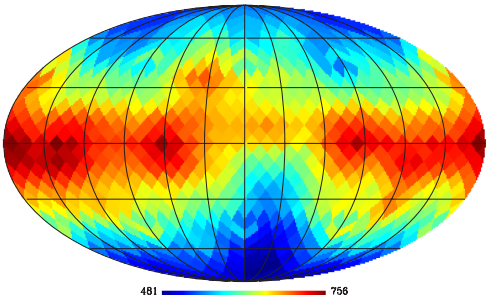

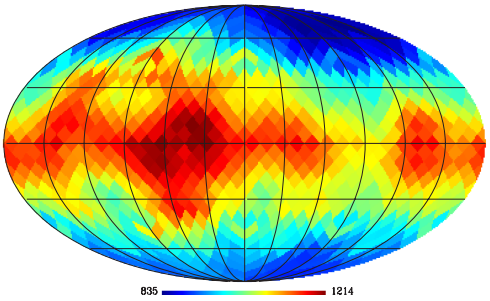

Figure 2. These sky maps, in Galactic coordinates and from top to bottom panel, represent the mean of 100 σ-maps–MC obtained from a similar number of MC computed considering three cases: $B_0 = 0$, 10, and 30 nG, respectively, and with the magnetic field pointing in the SGP–NGP direction, which means that the equator is the preferred plane. Note that for $B_0 \neq 0$, the region around the equator concentrates strong angular correlations, here represented by the intense and large red sky patches.

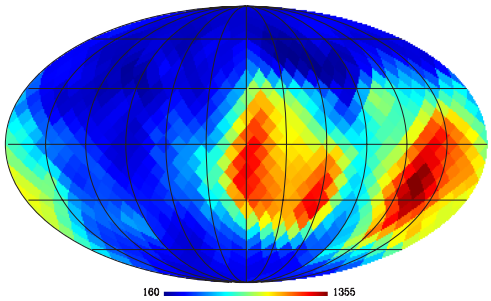

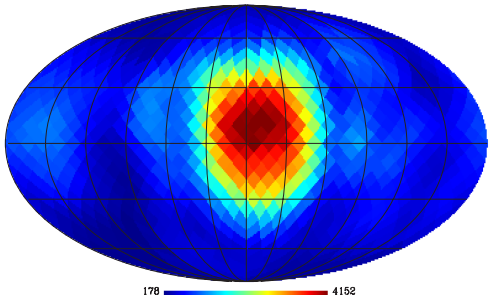

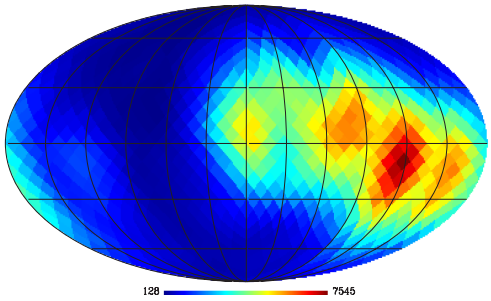

Figure 3. For illustration, we show three σ-maps: the σ-map–*WMAP* from the ILC-5 yr CMB map (top panel), and two σ-maps–MC having large dipole term S_1 one obtained from a MC map with $B_0 = 10$ nG (middle panel) and the other obtained from a MC map with $B_0 = 30$ nG (bottom panel).

Interestingly, simulations seems to indicate that an intensity of $B_0 \sim 15$ nG is enough to have a NS-symmetry as strong as *WMAP* data (see Fig. 4).

The effect of the magnetic field on the set of (ℓ, m) modes, for a given multipole ℓ, deserves a close inspection. We know that in the statistically isotropic case the power of the ℓ multipole in a CMB map, given by $C_\ell = (1/2\ell + 1)\sum_{m=-\ell}^{\ell} |a_{\ell m}|^2$, is uniformly distributed between the $(2\ell + 1)$ modes, for $m = -\ell, \ldots 0, \ldots \ell$. However, when a primordial magnetic field is acting on the CMB, and pointing in the SGP–NGP direction, we expect a non-uniform distribution of such power with a net predilection for the planar modes perpendicular to this axis, event that is termed the $m = \ell$-preference.

To investigate if the multipoles of our MC are experiencing this planarity phenomenon when $B_0 \neq 0$, we perform a probabilistic analysis of how the power of the quadrupole moment C_2 and octopole moment C_3 is distributed in their $(2\ell + 1) = 5$ and $(2\ell + 1) = 7$ modes, respectively. For this as a criterium for measuring the predilection for the (ℓ, m) mode, we consider those values obtained for the quadrupole and octopole from the ILC-5 yr CMB map, that is, (ℓ, m) is a preferred mode when it takes more than 35 per cent of the power of such multipole, i.e. $|a_{\ell m}|^2 + |a^*_{\ell m}|^2 > 0.35\,(2\ell + 1)\,C_\ell$. Given a subset of MC where the power of at least one of their $(2\ell' + 1)$ modes, of a given ℓ' multipole, is greater than $0.35\,(2\ell' + 1)\,C_{\ell'}$, we define $\mathcal{P}_{\ell' m'}$ as the probability that the mode (ℓ', m') satisfies the power distribution criterium (PDC): $|a_{\ell' m'}|^2 + |a^*_{\ell' m'}|^2 > 0.35\,(2\ell' + 1)\,C_{\ell'}$. For instance, $\mathcal{P}_{2,2}$ is the probability that the quadrupolar mode $(\ell', m') = (2, 2)$ satisfies $|a_{2,2}|^2 + |a^*_{2,2}|^2 > (0.35)(5)\,C_2$, where such probability is computed considering the subset of MC where at least one of the five modes (ℓ', m'), for $\ell' = 2$ and $m' = -2, -1, 0, 1, 2$, has power greater than $(0.35)\,(5)\,C_2$. We perform a comparative analysis for two sets of MC data, namely the set of 1000 MC ΛCDM (i.e. $B_0 = 0$, hereafter MC–ΛCDM) and the set of 1000 MC produced with $B_0 = 20$ nG (hereafter MC-B20).

Additionally, to realize a possible correlation between the quadrupole–octopole planes alignment and the NS-asymmetry phenomena, we also investigate the occurrence of the $m = \ell$-preference in three subsets of the MC–ΛCDM and MC-B20 sets, namely those subsets that satisfy the PDC for the quadrupole and the octopole simultaneously and such that their corresponding σ-maps–MC have (i) any dipole moment value $S_1^{\rm MC}$, hereafter denoted by MC–ΛCDM 0-SD and MC-B20 0-SD subsets, respectively; (ii) dipole moment value $S_1^{\rm MC}$ larger than the mean value plus one standard

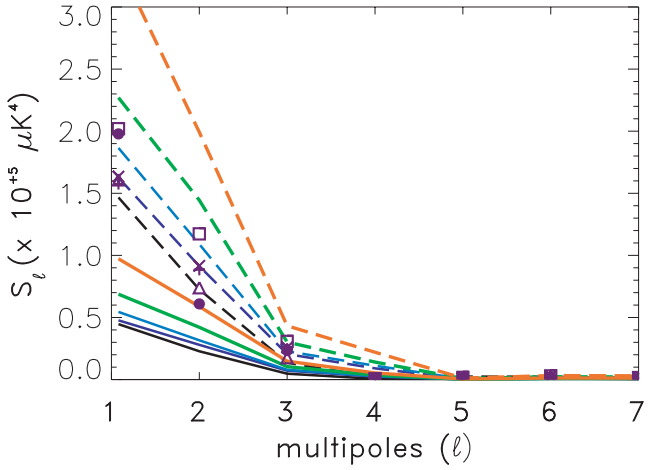

Figure 4. Angular power spectra of the σ-maps–MC for MC produced with different magnetic fields intensities together with the σ-maps–*WMAP* spectra. The plus, square, times, bullet and triangle symbols represent the data from the ILC-5 yr, HILC-5 yr, ILC-3 yr, PPG-3 yr and OT-3 yr CMB maps, respectively. From bottom to top, the solid (dashed) lines represent the mean (95 per cent CL) values computed from the set of σ-maps–MC corresponding to the cases $B_0 = 0, 10, 15, 20, 30$ nG, respectively.

deviation, hereafter these data are termed MC–ΛCDM 1-SD and MC-B20 1-SD, respectively, and (iii) dipole moment value $S_1^{\rm mc}$ larger than the mean value plus two standard deviations, hereafter these data are termed MC–ΛCDM 2-SD and MC-B20 2-SD, respectively. The fraction of MC, in the MC–ΛCDM and MC-B20 sets, that satisfies the above PDC for the quadrupole and the octopole simultaneously is ∼0.63 for all these data subsets.

Our results for these computations are shown in Table 1, where we observe the following results. First, as expected for the three sets of MC–ΛCDM data, the analysis reveals that the quadrupole and the octopole have their power uniformly distributed between all the (ℓ, m) modes. Secondly, regarding the MC-B20 data sets, it is observed a weak preference for the $(\ell, m) \neq (\ell, 0)$ modes in 0-SD and 1-SD data sets, while the planarity or $m = \ell$-preference is actually evident in the set 2-SD. Due to this fact, and according to the definition of $\mathcal{P}_{\ell m}$, we conclude that there is a net correlation between the quadrupole–octopole planes alignment (represented by the $m = \ell$-preference through the large values of $\mathcal{P}_{2,2}$ and $\mathcal{P}_{3,3}$) and the NS-asymmetry phenomena (represented by the fact that these large probability values appear only considering those MC that produce σ-maps–MC with the largest dipoles $S_1^{\rm MC}$). We understand this $m = \ell$-preference as a consequence of the planarity induced by the preferred direction settled by the magnetic field, as illustrated with two examples in Fig. 5. Additionally, one notes the effect that this planarity produces in the σ-maps–MC causing a concentration of strong angular correlations (red regions) around the equator, which is the preferred plane, as clearly seen in the mean of the σ-maps–MC skies showed in Fig. 2.

An important part of our analyses is the robustness tests. To assert the robustness of our results when using a different set of parameters in the σ-map method, we investigated the effect of changing $\gamma_0, N_{\rm bins}, N_{\rm caps}$ and $N_{\rm side}$ of the CMB map in analysis, in the computation of the σ-maps. For this, we performed several σ-map calculations using spherical caps of $\gamma_0 = 45^\circ, 60^\circ$ of aperture, $N_{\rm bins} = 45, 60, 90$ and $N_{\rm caps} = 768, 3\,072$, resulting in minor differences in all these cases. Additionally, we also examine the influence of the angular resolution of the CMB maps by computing the σ-maps considering different pixelization parameters of the CMB maps, namely $N_{\rm side} = 16$ and 32. In particular, the σ-maps showed in Fig. 2, plotted in Galactic coordinates, and their corresponding angular power spectra analyses in Fig. 1, were calculated using $\gamma_0 = 45^\circ$, $N_{\rm bins} = 45$, $N_{\rm caps} = 768$ and $N_{\rm side} = 32$. Summarizing, our robustness tests show that using a set of parameters within a certain range of values, we obtain results that are fully consistent with those showed in Fig. 4.

5 CONCLUSIONS

We investigated a plausible primordial scenario where a homogeneous magnetic field acting on the photon–baryon fluid at the recombination era, introduces a preferred direction that establish a statistical isotropy breaking. This setting offers a possible explanation for those anomalies found in *WMAP* data that seems to be associated to a preferred axis in the space, like the hemispherical NS-asymmetry and the planarity of some CMB low-order multipoles (where such a plane is perpendicular to that axis). It is found that this magnetic field induces correlations between the CMB multipoles, manifested through non-diagonal terms in the multipole correlation matrix (see equations 7–9). Accordingly, we have simulated five sets of CMB skies considering an equal number of strengths B_0 of the magnetic field. These MC CMB maps, with multipoles in the range $\ell = 2$–10, are used to investigate their large-angle correlations using our σ-map method. With these data sets, we performed a quantitative analysis of their large-angle signatures and perform a comparison with similar features computed from *WMAP* maps. For this, we consider a set of full-sky cleaned CMB maps, obtained from 5- and 3-yr *WMAP* data releases, namely the ILC-5 yr,

Table 1. Probability comparative analyses of the power distribution for the $a_{\ell m}$ modes of the quadrupole ($\ell = 2$) and the octopole ($\ell = 3$) in those subsets of MC–ΛCDM and MC-B20 that satisfies the PDC for the quadrupole and octopole simultaneously. The probability $P_{\ell m}$ is defined in the text. 0-SD means that we are consider for analysis the subset of the MC sets (mentioned above) such that their corresponding σ-maps–MC have any dipole moment value $S_1^{\rm mc}$; 1-SD (2-SD) means that we are consider for analysis the subset of the MC sets (mentioned above) such that their corresponding σ-maps–MC have dipole moment value $S_1^{\rm mc}$ larger than the mean value plus one (two) standard deviation(s).

MC data\$P_{\ell m}$	$P_{2,0}$ (per cent)	$P_{2,1}$ (per cent)	$P_{2,2}$ (per cent)	$P_{3,0}$ (per cent)	$P_{3,1}$ (per cent)	$P_{3,2}$ (per cent)	$P_{3,3}$ (per cent)
MC–ΛCDM 0-SD	26.7	39.0	34.3	26.3	23.8	26.6	23.3
MC–ΛCDM 1-SD	25.8	39.9	34.3	25.9	22.4	27.9	23.8
MC–ΛCDM 2-SD	30.2	32.6	37.2	20.2	26.6	26.6	26.6
MC–B20 0-SD	10.4	45.0	44.6	13.0	29.7	27.6	29.7
MC–B20 1-SD	11.4	39.3	49.3	7.5	31.9	25.3	35.3
MC–B20 2-SD	4.0	32.0	64.0	0.0	14.3	28.6	57.1

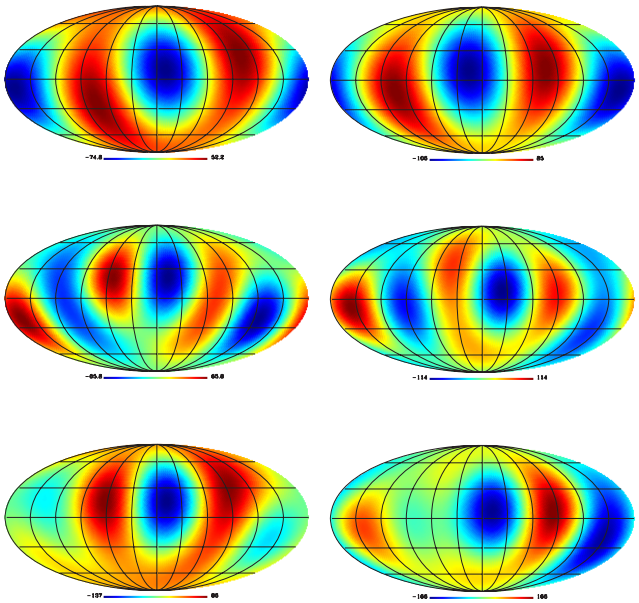

Figure 5. The left-hand (right hand) panels are the quadrupole $\ell = 2$, the octopole $\ell = 3$ and their sum $\ell = 2 + 3$ corresponding to the MC CMB map that produces the σ-map–MC plotted in the middle (bottom) panel of Fig. 3.

KCN-5 yr, ILC-3 yr, OT-3 yr and PPG-3yr maps, which were differently processed in order to account for foregrounds and systematic errors.

Our results can be summarized as follows. First, our analyses corroborate that an uneven hemispherical distribution in the power of the large-angular correlations, best known as NS-asymmetry phenomenon, is present in all these *WMAP* maps at more than 95 per cent CL as compared with statistically isotropic CMB maps produced according to the ΛCDM cosmological model (i.e. $B_0 = 0$). Secondly, we found that this hemispherical asymmetry phenomenon, is such that higher is the value of the field strength B_0, greater is the probability that such asymmetry be present in the MC CMB maps, and be revealed with a high dipole value $S_1^{\rm mc}$ in its corresponding σ-map–MC. In other words, our results show that the correlations introduced by a magnetic field mechanism in low-order CMB multipoles, for a sufficiently intense field, reproduce the NS asymmetry present in *WMAP* data as a common phenomena and not as an anomalous one. Thirdly, as expected, the MC CMB maps with $B_0 \neq 0$ exhibit the planarity effect in their low-order multipoles (see, for illustration, Fig. 5) as quantified in the Table 1, where the ℓ multipole power is concentrated in the $m = \pm\ell$ modes, and as evidenced by the intense red spots representative of strong angular correlations appearing in the equatorial region of the σ-maps–MC (see, for illustration, Fig. 2). Fourth, as shown in the Table 1, we found a significant correlation between the NS-asymmetry and quadrupole–octopole (planarity and) alignment phenomena. For completeness, we have also verified that our results are robust under different sets of parameters, as mentioned in the previous section, involved in the σ-map method calculations.

The large angular scales CMB anomalies challenge the statistical isotropy expected in the ΛCDM concordance model. Our results suggest that perhaps some of them could be suitable explained by just one physical phenomenon. As a matter of fact, there are several attempts to find the origin of large-angle CMB anomalies, but further investigations are needed to fully comprehend if they have one or more causes. In this sense, statistically anisotropic models explaining several anomalies with a minimum set of hypothesis should be explored.

We believe that our results will motivate the study of other statistically anisotropic scenarios, in particular, those where correlations between CMB anomalies appear. The magnetic field scenario analysed here is just the simplest one, and considering more realistic fields new effects could be present on the CMB temperature and polarization data (see e.g. Kosowsky & Loeb 1996; Seshadri & Subramanian 2001; Subramanian, Seshadri & Barrow 2003; Kahniashvili & Ratra 2005; Giovannini 2006, 2007; Giovannini & Kunze 2007, and references therein). In the same form, as well, possible relationships between these new effects and statistically anisotropic phenomena found in *WMAP* data could be established, all this deserving a better investigation.

ACKNOWLEDGMENTS

We are grateful for the use of the Legacy Archive for Microwave Background Data Analysis (LAMBDA). We also acknowledge the use of CMBFAST (http://www.cmbfast.org) developed by U. Seljak and M. Zaldarriaga. Some of the results in this paper have been derived using the HEALPix package (Górski et al. 2005). WSHR acknowledges financial support from the Brazilian Agency CNPq, process 150839/2007-3; AB acknowledges a PCI/DTI (MCT-CNPq) fellowship. We thank T. Villela, C. A. Wuensche, I. S. Ferreira and G. I. Gomero for insightful comments and suggestions. WSHR is grateful to FAPES, and to J. C. Fabris and the Gravitation and Cosmology Group at UFES for the opportunity to work there.

REFERENCES

Abramo L. R., Bernui A., Ferreira I. S., Villela T., Wuensche C. A., 2006a, Phys. Rev. D, 74, 063506
Abramo L. R., Sodré L., Jr, Wuensche C. A., 2006b, Phys. Rev. D, 74, 083515
Ackerman L., Carroll S. M., Wise M. B., 2007, Phys. Rev. D, 75, 083502
Adams J., Danielsson U. H., Grasso D., Rubinstein H., 1996, Phys. Lett. B, 253, 388
Aurich R., Lustig S., Steiner F., 2005, Class. Quantum Grav., 22, 3443
Barrow J. D., Ferreira P. G., Silk J., 1997, Phys. Rev. Lett., 78, 3610
Baym G., Bodeker D., McLerran, 1996, Phys. Rev. D, 53, 662
Bennett C. L. et al., 2003a, ApJS, 148, 1
Bennett C. L. et al., 2003b, ApJS, 148, 97
Bernui A., Villela T., Wuensche C. A., Leonardi R., Ferreira I., 2006a, A&A, 454, 409
Bernui A., Tsallis C., Villela T., 2006b, Phys. Lett. A, 356, 426
Bernui A., Tsallis C., Villela T., 2007a, Europhys. Lett., 78, 19001
Bernui A., Mota B., Rebouças M. J., Tavakol R., 2007b, A&A, 464, 479
Bernui A., Mota B., Rebouças M. J., Tavakol R., 2007c, Int. Journal of Mod. Phys. D, 16, 411
Bielewicz P., Górski K. M., Banday A. J., 2004, MNRAS, 355, 1283
Bielewicz P., Eriksen H. K., Banday A. J., Górski K. M., Lilje P. B., 2005, ApJ, 635, 750
Bunn E. F., 2007, Phys. Rev. D, 75, 083517
Campanelli L., Cea P., Tedesco L., 2006, Phys. Rev. Lett.,, 97, 131302 [Erratum-ibid. 97, 209903 (2006)]
Campanelli L., Cea P., Tedesco L., 2007, Phys. Rev. D, 76, 063007
Clarke T. E., Kronberg P. P., Boehringer H., 2001, ApJ, 547, L111
Copi C. J., Huterer D., Starkman G. D., 2004, Phys. Rev. D, 70, 043515
Copi C. J., Huterer D., Schwarz D. J., Starkman G. D., 2006, MNRAS, 367, 79
Copi C. J., Huterer D., Schwarz D. J., Starkman G. D., 2007, Phys. Rev. D, 75, 023507

Cresswell J. G., Liddle A. R., Mukherjee P., Riazuelo A., 2006, Phys. Rev. D, 73, 041302
Cruz M., Martínez-González E., Vielva P., Cayón L., 2005, MNRAS, 356, 29
Cruz M., Tucci M., Martínez-González E., Vielva P., 2006, MNRAS, 369, 57
Cruz M., Martínez-González E., Vielva P., Cayón L., 2007, ApJ, 655, 11
Chen G., Mukherjee P., Kahniashvili T., Ratra B., Wang Y., 2004, ApJ, 611, 655
Cheng B., Olinto A. V., 1994, Phys. Rev. D, 50, 2421
Chiang L.-Y., Naselsky P. D., Verkhodanov O. V., Way M. J., 2003, ApJ, 590, L65
Chiang L.-Y., Coles P., Naselsky P. D., Olesen P., 2007, JCAP, 1, 21
Demiański M., Doroshkevich A. G., 2007, Phys. Rev. D, 75, 123517
de Oliveira-Costa A., Tegmark M., 2006, Phys. Rev. D, 74, 023005
de Oliveira-Costa A., Tegmark M., Zaldarriaga M., Hamilton A., 2004, Phys. Rev. D, 69, 063516
Donoghue E. P., Donoghue J. F., 2005, Phys. Rev. D, 71, 043002
Donoghue J. F., Dutta K., Ross A., 2007, preprint(arXiv:0703455)
Dunkley J. et al., 2008, preprint (arXiv:0803.0586)
Durrer R., Kahniashvili T., Yates A., 1998, Phys. Rev. D, 58, 123004
Dvorkin C., Peiris H. V., Hu W., 2008, Phys. Rev. D, 77, 063008
Eriksen H. K., Hansen F. K., Banday A. J., Górski K. M., Lilje P. B., 2004a, ApJ, 605, 14; Erratum, 2004a, ApJ, 609, 1198
Eriksen H. K., Banday A. J., Górski K. M., Lilje P. B., 2004b, ApJ, 612, 633
Eriksen H. K., Banday A. J., Górski K. M., Lilje P. B., 2005, ApJ, 622, 58
Eriksen H. K., Banday A. J., Górski K. M., Hansen F. K., Lilje P. B., 2007, ApJ, 660, L81
Giovannini M., 2006, Phys. Rev. D, 74, 06302
Giovannini M., 2007, Phys. Rev. D, 76, 103508
Giovannini M., Kunze K. E., 2008, Phys. Rev. D, 77, 063003
Gold B. et al., 2008, preprint (arXiv:0803.0715)
Ghosh T., Hajian A., Souradeep T., 2007, Phys. Rev. D, 75, 083007
Gordon C., Hu W., Huterer D., Crawford T., 2005, Phys. Rev. D, 72, 103002
Górski K. M., Hivan E., Banday A., J., Wandelt B. D., Hansen F. K., Reinecke M., Bartlemann M., 2005, ApJ, 622, 759
Gümrükçüoğlu A. E., Contaldi C. R., Peloso M., 2007, JCAP, 11, 005
Hajian A., Souradeep T., 2003, ApJ, 597, L5
Hajian A., Souradeep T., 2005, preprint (arXiv:0501001)
Hajian A., Souradeep T., 2006, Phys. Rev. D, 74, 123521
Hajian A., Souradeep T., Cornish T., 2004, ApJ, 618, L63
Hansen F. K., Banday A. J., Górski K. M., 2004a, MNRAS, 354, 641
Hansen F. K., Cabella P., Marinucci D., Vittorio N., 2004b, ApJ, 607, L67
Helling R. C., Schupp P., Tesileanu T., 2006, Phys. Rev. D, 74, 063004
Hinshaw G. et al., 2003a, ApJS, 148, 135
Hinshaw G. et al., 2003b, ApJS, 148, 63
Hinshaw G. et al., 2007, ApJS, 170, 288
Hinshaw G. et al., 2008, preprint (arXiv:0803.0732)
Huterer D., 2006, New Astron. Rev., 50, 868
Hipólito-Ricaldi W. S., Gomero G. I., 2005, Phys. Rev. D, 72, 103008
Jaffe T. R., Banday A. J., Eriksen H. K., Górski K. M., Hansen F. K., 2006, A&A, 460, 393
Jarosik N. et al., 2007, ApJS, 170, 263
Kahniashvili T., Ratra B., 2005, Phys. Rev. D, 71, 103006
Kahniashvili T., Maravin Y., Kosowsky A., 2008, preprint (arXiv:0806.1876)
Kibble T. W., Vilekin A., 1995, Phys. Rev. D, 52, 679
Kim J., Naselsky P., Christensen P. R., 2008, Phys. Rev. D, 77, 13002
Koivisto T., Mota D. F., 2008a, JCAP, 06, 018
Koivisto T. S., Mota D. F., 2008b, preprint (arXiv:0805.4229)
Komatsu E. et al., 2008, preprint (arXiv:0803.0547)
Kosowsky A., Loeb A., 1996, ApJ, 461, 1
Krause M., Beck R., Hummel E., 1989, A&A, 217, 17
Kulsrud R. M., Anderson S. W., 1992, ApJ, 396, 606
Land K., Magueijo J., 2005a, MNRAS, 357, 994
Land K., Magueijo J., 2005b, Phys. Rev. Lett., 95, 071301
Land K., Magueijo J., 2006, MNRAS, 367, 1714
Land K., Magueijo J., 2007, MNRAS, 378, 153
López-Corredoira M., 2007, J. Astrophys. Astr., 28, 101
McEwen J. D., Hobson M. P., Lasenby A. N., Mortlock D. J., 2006, MNRAS, 371, L50
Mukhanov V., 2005, Physical Foundations of Cosmology. Cambridge Univ. Press, Cambridge
Nolta M. R. et al., 2008, preprint (arXiv:0803.0593)
Naselsky P., Kim J., 2008, preprint (arXiv:0804.3467)
Padmanabhan T., 1993, Structure Formation in the Universe. Cambridge Univ. Press, Cambridge
Park C.-G., Park C., Gott J. R., III, 2007, ApJ, 660, 959
Parker E. N., 1971, ApJ, 163, 255
Pereira T. S., Pitrou C., Uzan J.-P., 2007, JCAP, 09, 006
Piddington J. H., 1970, Aust. J. Phys., 23, 731
Pitrou C., Pereira T. S., Uzan J.-P., 2008, JCAP, 04, 004
Pullen A. R., Kamionkowski M., 2007, Phys. Rev. D, 76, 103529
Quashnock J., Loeb A., Spergel D. N., 1989, ApJ, 344, L49
Rakić A., Schwarz D. J., 2007, Phys. Rev. D, 75, 103002
Schwarz D. J., Starkman G. D., Huterer D., Copi C. J., 2004, Phys. Rev. Lett., 93, 221301
Seljak U., Zaldarriaga M., 1996, ApJ, 469, 437
Seshadri T. R., Subramanian K., 2001, Phys. Rev. Lett., 87, 101301
Souradeep T., Hajian A., 2004, Pramana, 62, 793
Souradeep T., Hajian A., 2005, preprint (arXiv:0502248)
Souradeep T., Hajian A., Basak S., 2006, New Astron. Rev., 50, 889
Spergel D. N. et al., 2007, ApJS, 170, 377
Subramanian K., Seshadri T. R., Barrow J. D., 2003, MNRAS, 344, L31
Tegmark M., de Oliveira-Costa A., Hamilton A. J. S., 2003, Phys. Rev. D, 68, 123523
Vachaspati T., 1995, Phys. Lett. B, 265, 258
Vainshtein S. I., Ruzmaikin A. A., 1972, Soviet. Astron., 15, 714
Vainshtein S. I., Zel'dovich Ya. B., 1972, Soviet. Phys. Uspekhi., 15, 159
Vielva P., Martínez-González E., Barreiro R. B., Sanz J. L., Cayón L., 2004, ApJ, 609, 22
Vielva P., Wiaux Y., Martínez-González E., Vandergheynst P., 2006, New Astron. Rev., 50, 880
Vielva P., Wiaux Y., Martínez-González E., Vandergheynst P., 2007, MNRAS, 381, 932
Weeks J. R., 2004, preprint (arXiv:0412231)
Wiaux Y., Vielva P., Martínez-González E., Vandergheynst P., 2006, Phys. Rev. Lett., 96, 151303
Wibig T., Wolfendale A. W., 2005, MNRAS, 360, 236
Widrow M., 2002, Rev. Mod. Phys, 74, 775
Wolfe A. M., Lanzetta K. M., Oren A. L., 1992, ApJ, 388, 17
Xu Y., Kronberg P. P., Habib S., Dufton Q. W., 2006, ApJ, 637, 19

This paper has been typeset from a TEX/LATEX file prepared by the author.